Label-free and redox proteomic analyses of the triacylglycerol-accumulating *Rhodococcus jostii* RHA1

José Sebastián Dávila Costa,[1] O. Marisa Herrero,[1,2] Héctor M. Alvarez[1] and Lars Leichert[3]

[1]Centro Regional de Investigación y Desarrollo Científico Tecnológico, Facultad de Ciencias Naturales, Universidad Nacional de la Patagonia, San Juan Bosco Km 4-Ciudad Universitaria, 9000 Comodoro Rivadavia (Chubut), Argentina

[2]Oil m&s, Av. Hipólito Yrigoyen 4250, 9000 Comodoro Rivadavia (Chubut), Argentina

[3]Ruhr-Universitat Bochum, Medizinisches Proteom-Center, Redox-Proteomics Group, Bochum, Germany

Correspondence

Héctor M. Alvarez

halvarez@unpata.edu.ar

Lars Leichert

lars.leichert@ruhr-uni-bochum.de

The bacterium *Rhodococcus jostii* RHA1 synthesizes large amounts of triacylglycerols (TAGs) under conditions of nitrogen starvation. To better understand the molecular mechanisms behind this process, we performed proteomic studies in this oleaginous bacterium. Upon nitrogen starvation, we observed a re-routing of the carbon flux towards the formation of TAGs. Under these conditions, the cellular lipid content made up more than half of the cell's dry weight. On the proteome level, this coincided with a shift towards non-glycolytic carbohydrate-metabolizing pathways. These pathways (Entner–Doudoroff and pentose-phosphate shunt) contribute NADPH and precursors of glycerol 3-phosphate and acetyl-CoA to lipogenesis. The expression of proteins involved in the degradation of branched-chain amino acids and the methylmalonyl-CoA pathway probably provided propionyl-CoA for the biosynthesis of odd-numbered fatty acids, which make up almost 30 % of RHA1 fatty acid composition. Additionally, lipolytic and glycerol-degrading enzymes increased in abundance, suggesting a dynamic cycling of cellular lipids. Conversely, abundance of proteins involved in consuming intermediates of lipogenesis decreased. Furthermore, we identified another level of lipogenesis regulation through redox-mediated thiol modification in *R. jostii*. Enzymes affected included acetyl-CoA carboxylase and a β-ketoacyl-[acyl-carrier protein] synthase II (FabF). An integrative metabolic model for the oleaginous RHA1 strain is proposed on the basis of our results.

INTRODUCTION

In recent years, increases in energy prices and concerns about environmental security and limited petroleum supplies have encouraged the search for renewable biofuels. Triacylglycerols (TAGs) are valuable raw materials for the production of biofuels, such as biodiesel. TAGs are traditionally produced from plants, e.g. oil seeds. However, the intensive use of agricultural land for the production of biofuels could potentially lead to food shortages and has already led to global increases in the prices of staple food. Thus, bacterial lipids can provide an attractive alternative raw material for biofuels.

Biosynthesis and accumulation of TAG is a common feature in bacteria of the genus *Rhodococcus* (Alvarez *et al.*, 1997; Alvarez & Steinbüchel, 2010). *Rhodococcus opacus* PD630 and *Rhodococcus jostii* RHA1 are considered oleaginous micro-organisms since they produce and store large amounts of TAGs (Alvarez & Steinbüchel, 2010). The latest advances in our understanding of fundamental aspects of TAG metabolism in these species are the consequence of the increased availability of genomic information for rhodococci (Chen *et al.*, 2013; Villalba *et al.*, 2013). In recent studies, different genes involved in TAG biosynthesis and accumulation in *R. opacus* PD630 and *R. jostii* RHA1 were identified, cloned and the associated proteins characterized. Two wax ester/diacylglycerol acyltransferase (WS/DGAT) enzymes (Atf1 and Atf2) from *R. opacus* PD630 were investigated in order to elucidate their *in vivo* role (Alvarez *et al.*, 2008; Hernández *et al.*, 2013). Furthermore, *in vitro* specificity of a WS/DGAT enzyme from *R. jostii* RHA1 faced

Abbreviations: ACP, acyl-carrier protein; FAS, fatty acid synthase; GAPDH, glyceraldehyde-3-phosphate dehydrogenase; LC, liquid chromatography; TAG, triacylglycerol; TCA, tricarboxylic acid.

Three supplementary figures and a supplementary table are available with the online Supplementary Material.

with diverse substrates was analysed (Barney *et al.*, 2012). MacEachran & Sinskey (2013) identified an NADPH-dependent glyceraldehyde-3-phosphate dehydrogenase (TadD). This enzyme is activated during TAG accumulation in *R. opacus* PD630 and required for the generation of NADPH for fatty acid biosynthesis under these conditions. Recently, we identified and characterized a phosphatidic acid phosphatase (PAP-type 2) that catalyses the dephosphorylation of phosphatidic acid to yield diacylglycerol as a substrate for TAG biosynthesis (Hernández *et al.*, 2014). Moreover, a novel ATP-binding cassette transporter functionally related to TAG metabolism in the oleaginous *R. jostii* RHA1 was identified (Villalba & Alvarez, 2014). Additionally, two structural proteins of the lipid bodies of strains *R. opacus* PD630 and *R. jostii* RHA1 were reported previously (MacEachran *et al.*, 2010; Ding *et al.*, 2012). Despite these mechanistic contributions, our understanding of lipid metabolism at an organismic level in rhodococci is still limited. Biosynthesis and accumulation of TAGs is a complex process that requires the concerted generation of precursors, reducing equivalents and energy for specific reactions. To unravel these processes, an integrated 'omics' study was performed recently in *R. opacus* PD630 during accumulation of lipids in order to understand the dynamics of lipid droplet formation in the cell (Chen *et al.*, 2014). This study included a transcriptomic analysis revealing the changes in gene expressions that lead to lipid accumulation. Additionally, the proteomic analysis of lipid droplets identified associated proteins (Chen *et al.*, 2014).

MS-based proteomics have become a powerful tool to elucidate and understand the mechanisms that underlie physiological processes (Le Bihan *et al.*, 2013; Liu *et al.*, 2014). Recent advances in liquid chromatography (LC), MS and the available evaluation software make label-free proteomic approaches feasible. We applied this approach to oleaginous bacteria to get a comprehensive overview of the metabolic adjustment of the cells during the transition from growth to lipid-accumulating stages. Furthermore, during the transition from cell growth to lipid accumulation, the cellular redox state needs to switch from an oxidative catabolism, consuming NADH to gain energy, to a reducing anabolism using NADPH to produce fatty acids. Oxidative modification of proteins often causes irreparable damage. However, not all protein oxidations are irreversible and thus damaging. Particularly, oxidation of the thiol-group of the amino acid cysteine present in proteins can be reversed by dedicated antioxidant systems *in vivo*, such as the thioredoxin or glutaredoxin system (Leichert, 2011). Recently, it has become apparent that oxidative thiol modifications play an important role in redox regulation and provide an effective mechanism for the modulation of the activity of redox-regulated proteins (Lindemann *et al.*, 2013; Müller *et al.*, 2013). The oxidation of such a redox-active cysteine can lead to structural changes and altered protein activity. Since the redox state of cells changes when they move from a growth stage to a TAG accumulation stage, we hypothesized that thiol-based redox-regulation

could be involved in this metabolic switch. In this sense the role of thiol-based redox regulation during this switch was assessed. We used an MS-based proteomic approach to assess the redox state of protein thiols that we developed (Leichert *et al.*, 2008). This approach is based on the differential modification of reduced and oxidized thiols in a complex protein sample with the ICAT reagent. We have previously used this technique in *Escherichia coli*, *Caenorhabditis elegans* and *Saccharomyces cerevisiae* to identify several putative redox-regulated proteins affecting a variety of cellular pathways (Leichert *et al.*, 2008; Brandes *et al.*, 2011; Kumsta *et al.*, 2011).

Knowledge of the metabolic pathways network and its possible redox regulation during TAG accumulation in oleaginous rhodococci is limited. Here we present a combined proteomic study to identify metabolic rearrangements and regulatory mechanisms in the oleaginous bacterium *R. jostii* RHA1 under lipid-accumulating conditions.

METHODS

Strain, culture media and growth conditions. *Rhodococcus jostii* RHA1 was grown at 28 °C and 200 r.p.m. in mineral salts medium (MSM) (Schlegel *et al.*, 1961). Sodium gluconate (1 %, w/v) was used as a carbon source. MSM supplemented with 1 g ammonium chloride l^{-1} (MSM1) was used to promote cellular growth, while MSM lacking ammonium chloride (MSM0) was used to induce lipid accumulation (Alvarez *et al.*, 2000). MSM0 supplemented with 10 mM methyl viologen (MSM0+MV) was included for redox proteomic studies. Generation time was calculated as the time that bacteria take to double in quantity during exponential phase.

Lipid analysis. The qualitative and semiquantitative analyses of intracellular lipids in *Rhodococcus* strains were performed by TLC. For intracellular analysis, 4–5 mg of lyophilized cells were extracted with a mixture of chloroform and methanol (2 : 1, v/v) for 120 min at 4 °C. Fifteen to thirty microlitres of extracts (depending on culture conditions) were separated by TLC, which was performed on silica-gel 60F254 plates (Merck) using hexane/diethyl ether/acetic acid (80 : 20 : 1, by vol.) as mobile phase. Tripalmitin (Fluka) and oleic acid (Fluka) were used as lipid reference substances. Lipid fractions were visualized after brief exposure to iodine vapour or UV light.

To determine the fatty acid content of the cell and the composition of lipids, 5–10 mg of dried whole cells was subjected to methanolysis in the presence of 15 % (v/v) sulfuric acid as described by Alvarez *et al.* (1996) and the resulting acyl methyl esters were analysed by GC using an HP 5890A gas chromatograph equipped with a FactorFour capillary column VF-23ms (30; 0.25; 0.25) and a flame-ionization detector. The injection volume was 0.2 ml, and helium (13 mm min^{-1}) was used as a carrier gas. A temperature programme was used for efficient separation of the methyl esters (80 °C 1 min, an initial ramp of 10 °C min^{-1} up to 160 °C, then an increase of 3 °C min^{-1} up to 200 °C, and a final ramp of 30 °C min^{-1} up to 240 °C maintained for 5 min to allow column cleaning). For quantitative analysis, tridecanoic acid was used as an internal standard.

Preparation of proteins for differential thiol trapping (OxICAT methodology). The thiol-trapping protocol established by Leichert *et al.* (2008) was followed. *R. jostii* RHA1 was inoculated in MSM1 and incubated overnight. Fresh MSM1 and MSM0 media were inoculated to an initial OD$_{600}$ of ~0.2 and incubated for 8 h at 28 °C. At that point, the MSM0 culture was split into subcultures. One

subculture was then supplemented with methyl viologen (10 mM) to induce oxidative stress. After 1 hour, 10 ml of culture in each medium (MSM1, MSM0 and MSM0 + MV) was diluted in fresh medium to an OD_{600} of ~0.4. For each sample, 0.4 ml of cell culture (corresponding to approximately 100 µg of cellular protein) was harvested by centrifugation (16 100 **g**, 4 °C, 10 min) and washed twice with anaerobic PBS, pH 7.4. The cell pellet was then resuspended in 80 µl of anaerobic denaturing buffer [6 M urea, 0.5 % (w/v) SDS, 10 mM EDTA, 200 mM Tris/HCl, pH 8.5] and the contents of one vial of cleavable light ICAT reagent (AB Sciex) dissolved in 20 µl acetonitrile were added. Cells were disrupted in this solution by sonication in a pre-chilled (4 °C) VialTweeter instrument (Hielscher Ultrasonics) with a cycle of 0.5 s at an amplitude of 90 % five times for 45 s, interrupted by a 1 min incubation on ice. Samples were then incubated at 1300 r.p.m. for 2 h at 37 °C in the dark. Proteins were precipitated by adding 400 µl pre-chilled (−20 °C) acetone and incubated overnight at −20 °C. Afterwards, samples were centrifuged (16 100 **g**, 4 °C, 30 min) and the protein pellet was washed twice by rinsing with 400 µl pre-chilled acetone. A thiol reduction step and labelling with heavy ICAT reagent followed and peptide purification was performed as described elsewhere (Leichert *et al.*, 2008; Lindemann & Leichert, 2012). Samples were stored at −80 °C until MS analysis.

Preparation of protein extracts for MS-based label-free quantitative proteomic analysis. *R. jostii* RHA1 was inoculated in MSM1 and incubated overnight. Fresh MSM1 and MSM0 media were inoculated (initial OD_{600} ~0.2) and incubated for 8 h at 28 °C. For each sample, 2 ml of cell culture were harvested by centrifugation (16 100 **g**, 4 °C, 10 min) and washed twice with washing buffer (25 mM Tris buffer pH 7, 2 mM EDTA). The cell pellet was then resuspended in 100 µl urea solution (6 M urea, 100 mM Tris, pH 7.8) and 5 µl reducing solution (200 mM DTT, 100 mM Tris, pH 7.8). Cells were disrupted by sonication as described above and incubated for 1 h at room temperature (RT) for complete denaturation. Subsequently, 20 µl reducing solution and 20 µl alkylation solution (200 mM iodoacetamide, 100 mM Tris, pH 7.8) were added to the samples; before and after the addition of the alkylation solution, samples were incubated for 1 h at RT. After centrifugation (16 100 **g**, 30 min), proteins were precipitated by adding 5 volumes of pre-chilled (−20 °C) acetone and incubated overnight at −20 °C. Samples were then centrifuged (16 100 **g**, 30 min, 4 °C) and the protein pellet was washed twice by rinsing with 500 µl pre-chilled (−20 °C) acetone. The protein pellet was dried, dissolved in 100 µl 0.04 M ammonium bicarbonate and digested with trypsin at 37 °C for between 14 and 16 h. The protein pellet was resuspended with a glass rod fitting the Eppendorf tube to enhance solution. After trypsin digestion, the concentration of peptides was determined and samples were stored at −80 °C until subjected to MS analysis.

LC-MS/MS analysis of protein extracts. LC-MS/MS experiments of at least three biologically independent replicates were performed. A sample (1.2 µl) containing 600 ng of peptides was dissolved in 30 µl 0.1 % trifluoroacetic acid. LC of 15 µl of the peptide sample was performed using an HP Ultimate 3000 system (Dionex) as described elsewhere (Lindemann *et al.*, 2013). Mass spectra were obtained online by an LTQ Orbitrap Velos instrument (Thermo Fisher Scientific); the 20 most intense peaks (minimal signal intensity 1500, charge range +2 to +4) in each MS spectrum were selected for MS/MS fragmentation with an exclusion time of 35 min.

Data analysis – protein quantification. Analysis of the data from free-label and redox proteomic analyses was performed using MaxQuant version 1.4.1.2 (Cox & Mann, 2008). MSM0 samples were compared to the corresponding MSM1 samples and to MSM0 + MV in the case of redox proteomes. Andromeda was used as peptide search engine and the protein database of *R. jostii* RHA1

from NCBI was used for peptide identification (Cox *et al.*, 2011). Proteins were considered significantly regulated when: (1) they showed on average an increase >2-fold in their abundance in MSM0; (2) the fold change was at least >1.5-fold in each of the individual biological replicates; (3) Student's *t*-test showed a *P* value below 0.05. *P* value was calculated using the T.TEST function of Excel version 2007 (Microsoft).

RESULTS AND DISCUSSION

R. jostii RHA1 growth in media with and without nitrogen source

To identify a time point for proteomic sample analysis, we monitored the growth of *R. jostii* RHA1 in media with (MSM1) and without nitrogen source (MSM0) for 34 h. Generation time in media containing 1 mM ammonium chloride as nitrogen source was 2.5 h. Cells reached stationary phase after 26 h of incubation (Fig. S1, available in the online Supplementary Material). As expected, *R. jostii* RHA1 showed a completely different growth behaviour in medium lacking a nitrogen source. Although the cell culture exhibited a slight increase of biomass between 2 and 10 h due to carry over of the nitrogen source (pre-culture cells were not washed before cell suspension in MSM0), stationary phase was reached already after 11 h of incubation in MSM0 (Fig. S1). While cell growth and production of biomass by *R. jostii* RHA1 was stimulated in nitrogen-source-containing media, cultivation of cells under nitrogen-limiting conditions promoted the biosynthesis and accumulation of TAGs. This is consistent with previous studies for rhodococci (Alvarez *et al.*, 1996; Alvarez & Steinbüchel, 2010). For further studies we decided to harvest cells 8 h after inoculation, since at this point *R. jostii* RHA1 was in exponential phase in both media (Fig. S1). Sampling during the exponential phase of growth should exclude modifications in the proteome due to a change in the phase of growth.

TAG accumulation and fatty acid content in *R. jostii* RHA1

To assess the fatty acid composition of *R. jostii* RHA1's lipids, and to determine the accumulation of TAGs, we analysed the total TAG content and quantified fatty acids using TLC and GC. The fatty acid profiling revealed hexadecanoic acid ($C_{16:0}$) and octadecenoic acid ($C_{18:1}$) as the predominant fatty acids occurring in *R. jostii* RHA1 as has been reported previously (Hernández *et al.*, 2008). In addition, odd-numbered chain-length fatty acids ($C_{15:0}$, $C_{17:0}$ and $C_{17:1}$) were produced (Fig. 1). Our analyses showed a higher TAG and total fatty acid content in cells grown in medium without nitrogen source in comparison with those cultivated in the presence of nitrogen (Fig. 1). However, the overall composition of fatty acids did not change significantly in response to nitrogen availability.

The presence of methyl viologen (paraquat) in the culture medium negatively affected TAG accumulation by *R. jostii* RHA1 (Fig. 1). This oxidative stressor also promoted a
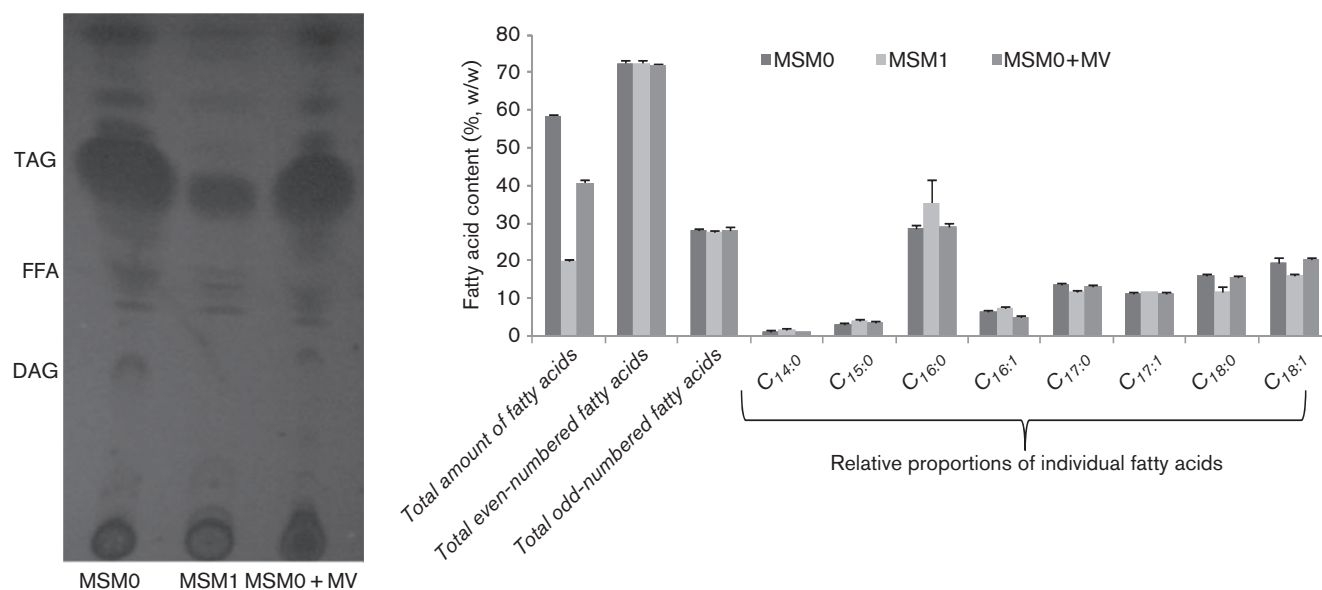
Fig. 1. Lipid analysis of whole-cell extracts of *R. jostii* RHA1. Total TAG content and quantification of fatty acids using (a) TLC and (b) GC. Total fatty acids are expressed as a percentage of cellular dry weight and the relative proportions of individual fatty acids are expressed as percentages (w/w). MSM0 (without nitrogen source), MSM1 (with nitrogen source), MSM0+MV (without nitrogen source+methyl viologen). FFA, free fatty acids; DAG, diacylglycerol.

dramatic decrease in TAG accumulation in cells of *R. opacus* PD630 cultivated under nitrogen-limiting conditions (Bequer Urbano *et al.*, 2013). We speculated that some proteins of the lipid biosynthesis and accumulation machinery may be sensitive to the redox changes promoted by the presence of methyl viologen in cells of those strains. In order to detect these redox-sensitive proteins involved in TAG biosynthesis and accumulation, we performed redox proteomic analyses using methyl viologen as pro-oxidant (see below).

Under nitrogen starvation *R. jostii* RHA1 switches its proteome towards pathways needed for TAG accumulation

To understand the changes in the proteome that cause TAG accumulation, we performed a global analysis of *R. jostii* RHA1's cellular proteins in the presence and absence of a nitrogen source in the culture media. We were able to detect about 2200 different proteins in *R. jostii* RHA1 protein extracts (Table S1). This constitutes approximately one-quarter of the predicted protein sequences in this strain (McLeod *et al.*, 2006). Among those proteins, only 108 passed our strict significance parameters (see Methods) between cells grown in the presence and absence of a nitrogen source (Table S1). We classified these proteins according to their physiological role (Table 1). This analysis revealed that specific metabolic pathways, such as the pentose phosphate pathway, the Entner–Duodoroff pathway, the methylmalonyl-CoA pathway, and amino acid degradation and glyceroneogenesis, the conversion of

precursors other than glycerol or glucose to glycerol 3-phosphate, were induced during TAG-accumulating conditions.

Glucose-degrading pathways that produce NADPH accommodate TAG accumulation

All proteins involved in the classical glycolytic Embden–Meyerhoff pathway as well as the gluconeogenesis pathway were detected in cells cultivated under both TAG-accumulating and regular conditions. However, abundance of phosphofructokinase (the enzyme catalysing the committed step of glycolysis), glucose-6-phosphate isomerase (glycolysis and gluconeogenesis) and fructose 1,6-bisphosphatase (gluconeogenesis), increased >2-fold under TAG-accumulating conditions (Table 1, Fig. 2). Presumably, however, the activity of these enzymes is regulated post-translationally to avoid futile cycling of metabolites (Desvergne *et al.*, 2006; Chubukov *et al.*, 2014). Furthermore, the abundance of glycogen phosphorylase (2.3-fold), glycogen debranching enzyme (2.1-fold) and phosphoglucomutase (5.9-fold), all involved in the degradation of glycogen to glucose 6-phosphate, increased as well (Table 1). *R. jostii* RHA1 synthesizes glycogen predominantly during the exponential growth phase (Hernández *et al.*, 2008). TAG accumulation induced by nitrogen starvation (MSM0 medium) coincides with a growth arrest, bringing cells into stationary phase (Fig. S1). We presume that under these conditions glucose 6-phosphate is mobilized from glycogen by *R. jostii* RHA1 to feed glucose-degrading pathways, which then enable the cells to accumulate TAG (Fig. 2).

Table 1. Upregulated proteins of *R. jostii* RHA1 in the absence of nitrogen (MSM0 medium)

Gene*	*t*-test (*P*)†	Protein name	Metabolic pathway‡/description	Intensity§		Fold change‖
				MSM0	MSM1	
Central metabolism						
RHA1_ro02367	0.02	KHG/KDPG aldolase	Entner–Doudoroff	74 998 000	17 876 166	4.1
RHA1_ro05865	0.01	Fructose 1,6-bisphosphatase	Gluconeogenesis	54 256 000	27 231 333	2
RHA1_ro01056	0.02	Glycogen debranching enzyme	Glycogenolysis	21 570 333	10 181 000	2.1
RHA1_ro01447	0.001	Glycogen phosphorylase	Glycogenolysis	23 149 000	9 908 000	2.3
RHA1_ro06413	0.01	Phosphoglucomutase	Glycogenolysis	9 618 466	1 612 066	5.9
RHA1_ro01448	0.005	Probable alpha amylase	Glycogenolysis	6 724 933	1 732 600	3.8
RHA1_ro06479	0.0002	6-Phosphofructokinase	Glycolysis	3 668 433	1 549 333	2.3
RHA1_ro05567	0.01	Glucose-6-phosphate isomerase	Glycolysis-gluconeogenesis	53 131 000	25 896 000	2
RHA1_ro04066	0.0008	Propionyl-CoA carboxylase	Methylmalonyl-CoA	9 039 400	4 481 700	2
RHA1_ro07233	0.006	Methylmalonyl-CoA mutase small subunit	Methylmalonyl-CoA	36 555 666	18 367 000	2
RHA1_ro07234	0.0005	Methylmalonyl-CoA mutase large subunit	Methylmalonyl-CoA	24 028 333	11 710 666	2
RHA1_ro02812	0.001	Xylulokinase	Pentose and glucuronate interconversions	1 701 433	0	Infinity
RHA1_ro05641	0.01	Glucose-6-phosphate dehydrogenase	Pentose phosphate	8 62 276	269 543	3.1
RHA1_ro07184	0.01	Glucose-6-phosphate dehydrogenase	Pentose phosphate	14 435 000	4 842 833	2.9
RHA1_ro03668	0.004	6-Phosphogluconate dehydrogenase	Pentose phosphate	4 351 866	888 633	4.8
RHA1_ro07185	0.0007	Transaldolase	Pentose phosphate	181 686 666	14 496 000	12.5
RHA1_ro07186	0.0008	Transketolase	Pentose phosphate	165 356 666	12 158 333	13.6
RHA1_ro02094	0.0003	Deoxyribose-phosphate aldolase	Pentose phosphate	1 595 466	225 053	7
RHA1_ro06111	0.003	Aldehyde dehydrogenase	Putative NAD(P)$^+$-dependent glyceraldehyde-3-phosphate dehydrogenase	2 111 066	1 035 866	2
RHA1_ro05599	0.0006	Aldehyde dehydrogenase	Putative NAD(P)$^+$-dependent glyceraldehyde-3-phosphate dehydrogenase	5 358 066	1 821 400	2.9
RHA1_ro06275	0.002	Aldehyde dehydrogenase	Putative NAD(P)$^+$-dependent glyceraldehyde-3-phosphate dehydrogenase	4 962 366	422 433	11.7
Fatty acid metabolism						
RHA1_ro03422	0.009	Probable fatty acid desaturase	Biosynthesis of unsaturated fatty acids	563 606	0	Infinity
RHA1_ro06265	0.004	FAD-dependent glycerol-3-phosphate dehydrogenase	Conversion of glycerol 3-phosphate to dihydroxyacetone phosphate. Gene: *glpD*	5 815 333	2 837 666	2
RHA1_ro06264	0.01	Glycerol kinase	Conversion of glycerol to glycerol 3-phosphate. Gene: *glpK*	2 724 800	1 349 100	2
RHA1_ro01426	0.02	Fatty acid synthase type I (FAS-I)	Fatty acid biosynthesis	1 390 366 667	349 516 666	3.9
RHA1_ro06095	0.005	Acetyl-CoA carboxylase	Fatty acid biosynthesis	2 118 000	220 006	9.6

Table 1. cont.

Gene*	t-test (P)†	Protein name	Metabolic pathway‡/description	Intensity§		Fold change‖
				MSM0	MSM1	
RHA1_ro01200	0.03	Acyl carrier protein	Fatty acid biosynthesis. FAS-II.	903 300 000	233 433 333	3.8
RHA1_ro01199	0.04	Malonyl-CoA-[ACP] transferase	Fatty acid biosynthesis. FAS-II. 'FabD'	38 107 666	14 286 833	2.6
RHA1_ro01201	0.04	β-Ketoacyl-[ACP] synthase	Fatty acid biosynthesis. FAS-II. 'FabF'	74 859 666	35 740 366	2
RHA1_ro05199	0.01	β-Ketoacyl-[ACP] reductase	Fatty acid biosynthesis. FAS-II. 'FabG'	17 878 366	4 738 933	3.7
RHA1_ro02340	0.0003	β-Ketoacyl-[ACP] reductase	Fatty acid biosynthesis. FAS-II. 'FabG'	15 993 533	6 066 500	2.6
RHA1_ro00189	0.00005	Acyl-CoA synthetase	Fatty acid degradation	38 120	0	Infinity
RHA1_ro01121	0.03	Long-chain-fatty-acid–CoA ligase	Fatty acid degradation	6 606 933	1 914 933	3.4
RHA1_ro03099	0.003	Esterase/lipase	Glycerolipid metabolism	1 660 966	638 613	2.6
RHA1_ro07162	0.01	Possible lipase	Glycerolipid metabolism	8 314 766	0	Infinity
RHA1_ro05180	0.0004	Phosphoenolpyruvate carboxykinase	Glyceroneogenesis	157 340 000	46 553 333	3.3
RHA1_ro06505	0.01	Glycerol-3-phosphate dehydrogenase [NAD(P)$^+$]	Glyceroneogenesis. Gene: gpsA	20 011 666	9 838 666	2
RHA1_ro02159	0.03	Phosphatidylserine decarboxylase proenzyme	Glycerophospholipid metabolism	4 590 866	895 533	5
RHA1_ro02104	0.01	Conserved hypothetical protein	Homologue protein of TadA from R. opacus PD630	2 153 700 000	929 196 666	2.3
RHA1_ro01601	0.001	Diacylglycerol acyltransferase (DGAT)	Kennedy pathway	2 246 366	915 676	2.4
RHA1_ro01115	0.04	1-Acylglycerol-3-phosphate O-acyltransferase (AGPAT)	Kennedy pathway	12 602 633	4 432 966	2.8
RHA1_ro04047	0.003	1-Acylglycerol-3-phosphate O-acyltransferase (AGPAT)	Kennedy pathway	13 928 333	6 975 700	2
RHA1_ro02025	0.01	1-Acylglycerol-3-phosphate O-acyltransferase (AGPAT)	Kennedy pathway	2 185 433	878 115	2.4
RHA1_ro02057	0.01	1-Acylglycerol-3-phosphate O-acyltransferase (AGPAT)	Kennedy pathway	2 104 866	410 686	5.1
RHA1_ro04207	0.04	Cyclopropane-fatty-acyl-phospholipid synthase	Phospholipid cyclopropane biosynthesis	24 169 333	11 790 466	2.1
RHA1_ro04839	0.00002	Cyclopropane-fatty-acyl-phospholipid synthase	Phospholipid cyclopropane biosynthesis	2 603 333	0	Infinity
RHA1_ro05863	0.03	Acyl-[acyl-carrier protein] desaturase	Polyunsaturated fatty acid biosynthesis	13 388 000	6 562 433	2
RHA1_ro01408	0.001	Linoleoyl-CoA desaturase	Polyunsaturated fatty acid biosynthesis	9 579 166	0	Infinity
RHA1_ro05100	0.002	Acyl-CoA dehydrogenase	β-Oxidation.	10 62 366	5 247 233	2
Amino acid and protein metabolism						
RHA1_ro05606	0.005	Probable putrescine oxidase	Arginine and proline metabolism	2 344 166	226 366	10.3
RHA1_ro00243	0.001	ATP-dependent Clp protease ATP-binding subunit	Degradation of proteins	139 206	0	Infinity
RHA1_ro05596	0.00002	Succinate-semialdehyde dehydrogenase [NAD(P)$^+$]	Glutamate, tyrosine and butanoate metabolism		0	Infinity
RHA1_ro05568	0.02	Succinate-semialdehyde dehydrogenase [NAD(P)$^+$]	Glutamate, tyrosine and butanoate metabolism	24 344 333	12 160 333	2
RHA1_ro05203	0.002	Butyryl-CoA dehydrogenase	Isoleucine degradation	8 982 700	3 292 733	2.7
RHA1_ro02860	0.0004	Enoyl-CoA hydratase	Isoleucine degradation	13 786 000	2 142 800	6.4
RHA1_ro03952	0.001	3-Hydroxyacyl-CoA dehydrogenase	Isoleucine degradation. β-Oxidation.	1 089 400	203 483	5.3
RHA1_ro04543	0.002	Succinate-semialdehyde dehydrogenase [NAD(P)$^+$]	L-Glutamine metabolism	72 753 333	7 940 966	9.1
RHA1_ro04544	0.02	4-Aminobutyrate transaminase	L-Glutamine metabolism	10 847 433	407 533	26.6

Table 1. cont.

Gene*	*t*-test (*P*)†	Protein name	Metabolic pathway‡/description	Intensity§		Fold change‖
				MSM0	MSM1	
RHA1_ro01405	0.001	Glutamate dehydrogenase (NADP$^+$)	L-Glutamine metabolism	8 918 033	3 733 266	2.3
RHA1_ro06016	0.0009	Glutamate decarboxylase.	L-Glutamine metabolism	2 115 433	806 733	2.6
RHA1_ro01564	0.03	Shikimate 5-dehydrogenase	Phenylalanine, tyrosine and tryptophan metabolism. Production of NADPH	5 256 700	807 200	6.5
RHA1_ro00907	0.01	Glycine cleavage system	System triggered in response to high concentrations of glycine. Production of NADPH	60 970 333	27 763 666	2.1
RHA1_ro01539	0.0003	3-Hydroxyisobutyrate dehydrogenase	Valine degradation. Production of NADPH	3 297 166	0	Infinity
RHA1_ro01542	0.007	Methylmalonate-semialdehyde dehydrogenase	Valine degradation. Production of NADPH	3 976 533	0	Infinity
Transporters						
RHA1_ro06004	0.01	ABC amino acid transporter, substrate binding component	ABC transport system permease protein ProV	5 381 033	1 442 100	3.7
RHA1_ro02126	0.007	Probable ABC amino acid transporter, substrate binding component	Amino acid/amide ABC transporter ATP-binding protein 2, HAAT family	27 650 000	0	Infinity
RHA1_ro04866	0.009	Phosphate transport system protein PhoU	Gene: *phoU2*	13 831 000	6 850 500	2
RHA1_ro00981	0.004	ABC amino acid transporter, ATP-binding component	Glutamine transport system	3 737 900	1 766 833	2.1
RHA1_ro06003	0.005	ABC amino acid transporter, ATP-binding component	Glutamine transport system ATP-binding protein	1 789 400	265 440	6.7
RHA1_ro00994	0.01	ABC branched-chain amino acid transport, ATP-binding component	Leucine/isoleucine/valine transporter subunit. Gene: *livF*	603 446	0	Infinity
RHA1_ro02130	0.01	ABC branched-chain amino acid transporter, ATP-binding component	Leucine/isoleucine/valine transporter subunit. Gene: *livF*	5 736 866	0	Infinity
RHA1_ro00993	0.00003	ABC branched-chain amino acid transport, ATP-binding component	Leucine/isoleucine/valine transporter subunit. Gene: *livG*	1 707 300	0	Infinity
RHA1_ro02129	0.002	ABC branched-chain amino acid transporter, ATP-binding component	Leucine/isoleucine/valine transporter subunit. Gene: *livG*	9 250 566	0	Infinity
RHA1_ro00991	0.000007	ABC branched chain amino acid transporter, permease component	Leucine/isoleucine/valine transporter subunit. Gene: *livH*	264 986	0	Infinity
RHA1_ro02128	0.0001	ABC branched amino acid transporter, permease component	Leucine/isoleucine/valine transporter subunit. Gene: *livM*	1 451 266	0	Infinity
RHA1_ro01893	0.02	ABC amino acid transporter, periplasmic binding protein	Polar amino acid transport system substrate-binding protein	17 190 333	1 580 183	10.8
Nitrogen metabolism						
RHA1_ro06530	0.00007	Ammonium transporter	Ammonium transmembrane transporter activity	7 558 266	0	Infinity
RHA1_ro06366	0.009	Nitrite reductase [NAD(P)H]	Large subunit	933 433	0	Infinity

Table 1. cont.

Gene*	t-test (P)†	Protein name	Metabolic pathway‡/description	Intensity§		Fold change‖
				MSM0	MSM1	
RHA1_ro00862	0.005	Nitrite reductase [NAD(P)H]	Large subunit, nasD gene	1 362 346	0	Infinity
RHA1_ro06531	0.004	Nitrogen regulatory protein P-II	Regulatory protein, glnB gene	161 203 333	14 511 066	11.1
RHA1_ro06532	0.00008	[Protein-PII] uridylyltransferase	Regulatory protein, glnD gene	8 483 600	0	Infinity
RHA1_ro06367	0.01	Nitrite reductase [NAD(P)H]	Small subunit	4 373 700	0	Infinity
RHA1_ro00863	0.000001	Nitrite reductase [NAD(P)H]	Small subunit, nasE gene	476 893	0	Infinity
RHA1_ro05678	0.000006	Urease gamma subunit	Urease complex, ureA gene	2 101 833	0	Infinity
RHA1_ro05679	0.0001	Urease beta subunit	Urease complex, ureB gene	2 012 000	0	Infinity
RHA1_ro05680	0.01	Urease alpha subunit	Urease complex, ureC gene	6 594 666	2 564 433	2.5
Transcriptional regulators						
RHA1_ro02425	0.007	Transcriptional regulator	ArsR family protein	753 230	123 493	6
RHA1_ro01553	0.004	Transcriptional regulator	GntR family protein	477 540	0	Infinity
RHA1_ro02131	0.007	Transcriptional regulator	GntR family protein	598 786	0	Infinity
RHA1_ro00765	0.01	Transcriptional regulator	IclR family protein	3 995 866	1 996 300	2
RHA1_ro02105	0.02	Transcriptional regulator	Possible regulator of TadA	2 252 500	1 099 633	2
Energy balance						
RHA1_ro02497	0.01	Alcohol dehydrogenase	Oxidation of alcohols. Production of NAD(P)H	5 622 933	1 615 433	3.4
RHA1_ro04873	0.0000007	Alcohol dehydrogenase	Oxidation of alcohols. Production of NAD(P)H	703 620	0	Infinity
RHA1_ro02119	0.003	NADP-dependent alcohol dehydrogenase	Oxidation of alcohols. Production of NADPH	1 730 033	179 780	9.6
RHA1_ro01880	0.0001	Aryl-alcohol dehydrogenase (NADP$^+$)	Oxidation of aromatic alcohols. Production of NADPH	679 790	217 043	3.1
RHA1_ro00348	0.0001	1-Pyrroline-5-carboxylate dehydrogenase	Oxidoreductase. Production of L-glutamate and NADPH or NADH	1 533 466	0	Infinity

ACP, acyl-carrier protein.

*According to the NCBI database.

†P value calculated using the T.TEST function of Excel version 2007 (Microsoft).

‡According to KEGG pathways database.

§Mean of Intensity LFQ values calculated by MaxQuant version 1.4.1.2 (Cox & Mann, 2008).

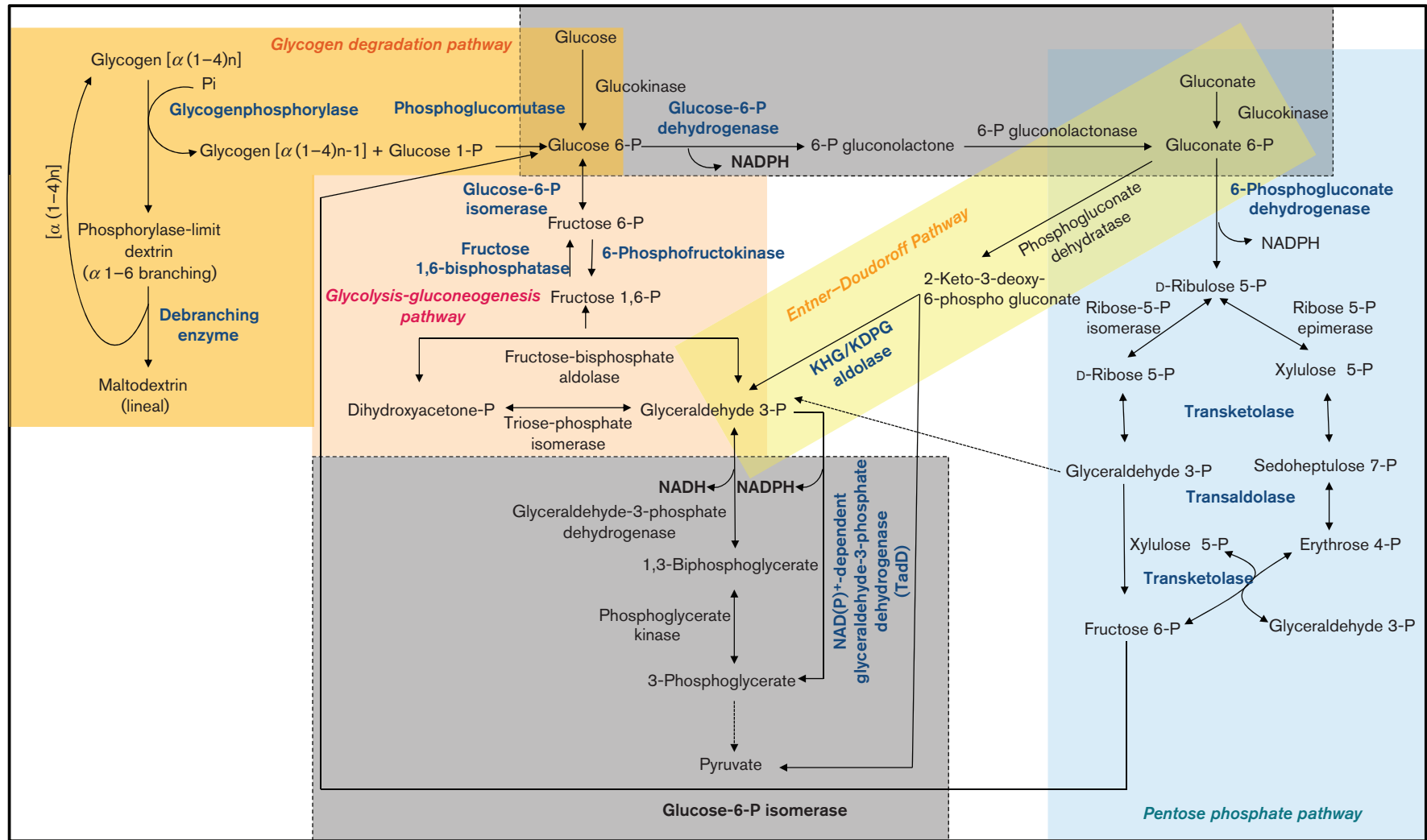‖Fold change designated 'Infinity' indicates that the protein was only detected in MSM0.

Fig. 2. Interaction of central metabolic pathways proposed for *R. jostii* RHA1. All enzymes were identified in the label-free proteome, but enzymes in blue showed significantly high abundance under TAG-accumulating conditions. P, phosphate.

Foremost, these are the alternative glucose metabolizing pentose phosphate and Entner–Doudoroff pathways, which showed significantly higher abundance under TAG-accumulating growth conditions (Table 1, Fig. 2). Unlike glycolysis, these pathways generate reducing equivalents in the form of NADPH, and not NADH. NADPH is a required cofactor for the biosynthesis of fatty acids.

During TAG accumulation, cells switch from NAD$^+$- to NADP$^+$-dependent glyceraldehyde-3-phosphate dehydrogenases

Additionally, both alternative glucose-degrading pathways produce glyceraldehyde 3-phosphate. This central metabolite could then be further metabolized NADH-dependently by glyceraldehyde-3-phosphate dehydrogenase (GAPDH) in the classical glycolytic pathway. However, some rhodococci have an alternative GAPDH, the so-called GAPDHN, capable of oxidizing glyceraldehyde 3-phosphate in an NADP$^+$-dependent manner. In the oleaginous strain R. opacus PD630, the TadD protein was identified to possess this activity (MacEachran & Sinskey, 2013). This enzyme was proposed as a key metabolic branch point between normal cellular growth and the TAG accumulation conditions; however, primary transcripts and abundance of this protein were never quantified. Our proteomic studies show a high abundance of three aldehyde dehydrogenases in R. jostii RHA1, when grown under TAG-accumulating conditions (Table 1). Bioinformatic analysis revealed that all three enzymes harbour the conserved motif typical for a GAPDHN (Fig. S2) (Iddar et al., 2005). In parallel, the NAD-dependent glyceraldehyde-3-phosphate dehydrogenase enzyme (ro03427) was decreased 2-fold (Table 2). This switch from NAD$^+$- to NADP$^+$-dependent glyceraldehyde 3-phosphate oxidation is central in the metabolic rearrangement of R. jostii RHA1's proteome.

Pyruvate is channelled into fatty acid biosynthesis on multiple levels

Pyruvate can be decarboxylated to acetyl-CoA, which can be utilized directly for the formation of malonyl-CoA by an acetyl-CoA carboxylase enzyme. Then, the multifunctional fatty acid synthase (FAS) utilizes these molecules as basic metabolites to produce acyl-CoA (Fig. 3). The abundance of acetyl-CoA carboxylase and the mammalian-like type FAS-I system was 9.6- and 3.9-fold under TAG-accumulating conditions, respectively (Table 1). The FAS-I system is a homo-dimer containing all the necessary domains to synthesize fatty acids of C$_{14}$–C$_{24}$ chain length (Gago et al., 2011; Smith et al., 2003). R. jostii RHA1 also utilizes a FAS-II system in which a fatty acyl chain is transferred between the active sites of dissociable component enzymes. FAS-II is involved in mycolic acid production by elongation of fatty acids produced by FAS-I (Sutcliffe et al., 2010). Three components of the FAS-II {malonyl-CoA-[acyl-carrier protein] (ACP) transferase, β-ketoacyl-[ACP] synthase and β-ketoacyl-[ACP] reductase} were identified with high abundance under TAG-accumulating conditions (Table

1). In addition, the high abundance of fatty acid desaturase enzymes detected under nitrogen starvation and normal growth conditions (Tables 1 and 2) may be responsible for the similar amount of unsaturated fatty acid in stored TAGs, such as C$_{16:1}$, C$_{17:1}$ and C$_{18:1}$ fatty acids (Fig. 1).

Additionally, our data suggests that pyruvate is also channelled into the glyceroneogenesis pathway, which catalyses the conversion of precursors other than glycerol or glucose to glycerol 3-phosphate (Hanson & Reshef, 2003) (Fig. 3), typically from pyruvate, glutamine, alanine or tricarboxylic acid (TCA) cycle intermediates (such as oxaloacetate). Pyruvate carboxylase and phosphoenolpyruvate carboxykinase enzymes are both involved in this pathway (Hanson & Reshef, 2003). Pyruvate carboxylase catalyses the conversion of pyruvate to oxaloacetate, while phosphoenolpyruvate carboxykinase produces the decarboxylation of oxaloacetate. Phosphoenolpyruvate carboxykinase activity catalyses the rate-limiting step in glyceroneogenesis (Hanson & Reshef, 2003). Pyruvate carboxylase (ro06517) was present in R. jostii RHA1 cells during cultivation under both regular and TAG-accumulating conditions, with a slightly (1.4-fold) higher abundance under TAG-accumulating conditions (Table S1). Phosphoenolpyruvate carboxykinase significantly increased its abundance 3.3-fold and the (NADP$^+$)-dependent glycerol-3-phosphate dehydrogenase (GpsA) was upregulated 2-fold under TAG-accumulating conditions (Table 1, Fig. 3). GpsA catalyses the synthesis of the final product of the glyceroneogenesis pathway, glycerol 3-phosphate, which can then be used for TAG biosynthesis (Fig. 3).

The TAG-assembling Kennedy pathway is upregulated under TAG-accumulating conditions

In rhodococci, TAGs are synthesized from fatty acids and glycerol 3-phosphate through the Kennedy pathway. This involves the sequential acylation of the sn-1,2 positions of glycerol 3-phosphate, and then the removal of the phosphate group and the final acylation step (Alvarez et al., 2012). Four 1-acylglycerol-3-phosphate O-acyltransferase (AGPAT) isoenzymes and one wax ester synthase/diacylglycerol acyltransferase (WS/DGAT) isoenzyme (ro01601) of the Kennedy pathway were highly synthesized by R. jostii RHA1 cells under nitrogen-limited TAG-accumulating conditions (Table 1, Fig. 3). Two additional WS/DGAT enzymes, ro05356 and ro06332, whose abundances were 1.4- and 1.8-fold higher under TAG-accumulating conditions, were detected in the proteome (Table S1). The highly synthesized ro01601 is the orthologue of Atf2, which is a WS/DGAT actively involved in TAG biosynthesis and accumulation in R. opacus PD630 (Hernández et al., 2013). The contribution of Atf2 to TAG accumulation in strain R. opacus PD630 is significant; an atf2-disrupted mutant exhibited a decrease in TAG accumulation down to 25–30 % (w/w) and an approximately 10-fold increase in glycogen formation in comparison with the wild-type strain (Hernández et al., 2013).

Table 2. Upregulated proteins of *R. jostii* RHA1 in the presence of nitrogen (MSM1 medium)

Gene*	*t*-test (*P*)†	Protein name	Metabolic pathway‡/description	Intensity§		Fold-change‖
				MSM1	**MSM0**	
RHA1_ro01103	0.01	Possible lipoprotein	Diacylglycerol lipase	661 843	0	Infinity
RHA1_ro00842	0.00005	Possible diacylglycerol kinase	Glycerolipid metabolism	310 956	0	Infinity
RHA1_ro03427	0.04	Glyceraldehyde-3-phosphate dehydrogenase	Glycolysis	16 633 667	7 987 066	2
RHA1_ro02122	0.001	Isocitrate lyase	Glyoxylate/dicarboxylate metabolism	278 046 667	84 429 333	3.2
RHA1_ro01307	0.0008	ʟ-Ectoine synthase	ʟ-Ectoine metabolism	43 849 333	1 046 380	41.9
RHA1_ro01244	0.000007	Possible lipase/esterase	Lipid degradation	775 106	0	Infinity
RHA1_ro02361	0.000006	Probable lipase	Lipid degradation	384 203	0	Infinity
RHA1_ro04204	0.00005	Acetyl-CoA C-acyltransferase	*β*-Oxidation	1 785 300	0	Infinity
RHA1_ro04205	0.04	Fatty oxidation complex	*β*-Oxidation	3 021 866	1 195 100	2.5
RHA1_ro06336	0.00005	Possible fatty acid desaturase	Polyunsaturated fatty acid biosynthesis	3 888 533	0	Infinity
RHA1_ro06335	0.004	Possible fatty acid desaturase	Polyunsaturated fatty acid biosynthesis	17 426 666	8 384 300	2
RHA1_ro05645	0.00008	ABC lipid A transporter	Ltp1 transports exogenous and endogenous long-chain fatty acids	157 493	0	Infinity

*According to the NCBI database.
†*P* value calculated using the T.TEST function of Excel version 2007 (Microsoft).
‡According to KEGG pathways database.
§Average of Intensity LFQ values calculated by MaxQuant version 1.4.1.2 (Cox & Mann, 2008).
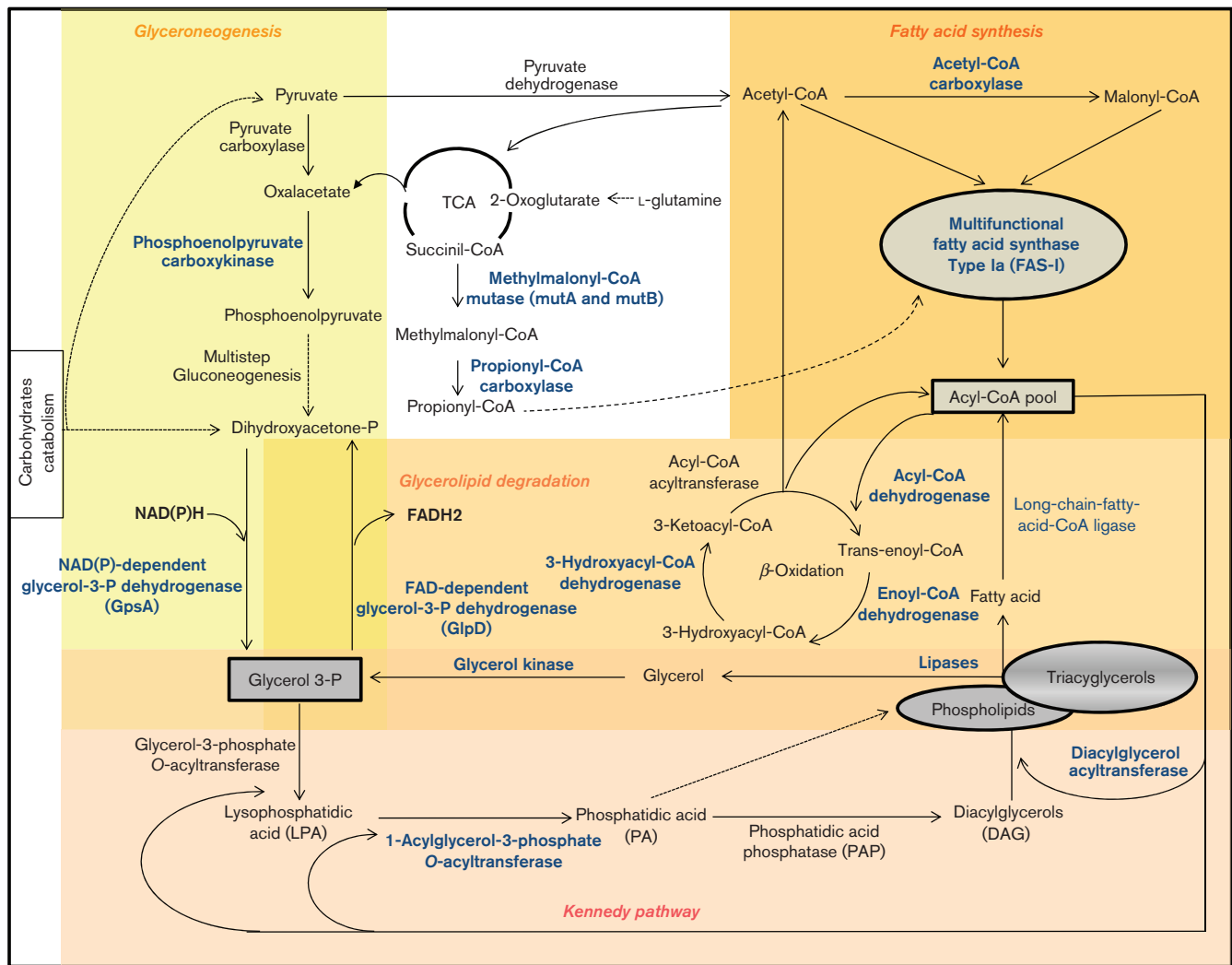‖Fold change designated 'Infinity' indicates that the protein was only detected in MSM1.

Fig. 3. Pyruvate is channelled into fatty acid biosynthesis on multiple levels. The acyl-CoA pool for TAG synthesis is mainly formed by the FAS-I system. All enzymes were identified in the label-free proteome, but enzymes in blue showed significantly high abundance under TAG-accumulating conditions. P, phosphate; TCA, tricarboxylic acid.

Certain TAG-degrading enzymes are present and even partially elevated under TAG-accumulating conditions

Strikingly, TAG degradation still seems to be active during lipid accumulation. The abundance of lipases encoded by genes *ro07162* and *ro03099* was increased under these conditions (Table 1). Lipases degrade TAG to fatty acids and glycerol. Moreover, some proteins involved in the β-oxidation of fatty acids were identified with a 2-fold higher abundance during TAG-accumulation in comparison with regular growth conditions (Table 1, Fig. 3). These results suggested that TAG recycling may occur to some extent in lipid-accumulating rhodococcal cells. The increase of TAG production by the oleaginous *R. opacus* PD630 during incubation of cells under storage conditions in the presence of an inhibitor of the lipolysis (Orlistat) supports this idea (M. S. Villalba & H. M. Alvarez, unpublished results). The

recycling process should involve mechanisms to metabolize the fatty acids and glycerol produced. Fatty acids might be re-esterified in order to rearrange 'old' TAGs. Glycerol released in these processes may be converted to dihydroxyacetone phosphate through the enzymes glycerol kinase (ro06264) and FAD-dependent glycerol-3-phosphate dehydrogenase (GlpD) (ro06265). Both enzymes significantly increased their abundances 2-fold under TAG-accumulating conditions (Table 1, Fig. 3). Transcriptomic analyses performed previously in *R. opacus* PD630 showed that genes encoding lipases, glycerol kinase and FAD-dependent glycerol-3-phosphate dehydrogenase were highly expressed in nitrogen-starvation in accordance with our results (Chen *et al.*, 2014). The simultaneous upregulation of the typically glycerol-3-phosphate degrading enzyme GlpD and the typically glycerol-3-phosphate synthesizing enzyme GpsA as mentioned above seems at first counter-intuitive. However,

these two enzymes form the glycerol-3-phosphate shuttle system in eukaryotic cells (Mráček *et al.*, 2013). This eukaryotic system recycles NAD$^+$, and while it is tempting to propose a similar role in the control of NADP$^+$ or glycerol 3-phosphate availability in oleaginous rhodococci, further studies are needed to elucidate the competing role of these enzymes under TAG-accumulating conditions.

The abundance of typical enzymes involved in TAG and fatty acid degradation is decreased under TAG-accumulating conditions

Some genes related to lipid metabolism significantly decreased their abundances in cells grown under TAG-accumulating conditions. Two lipases (ro01244 and ro02361), a diacylglycerol kinase enzyme (ro00842), enzymes of the β-oxidation pathway, and the isocitrate lyase enzyme (ro02122) exhibited a significantly higher abundance in cells growing under regular conditions (Table 2). Recently, we identified and characterized an ATP-binding cassette transporter (Ltp1) as an importer of long-chain fatty acid, which seems to play a functional role in lipid homeostasis in *R. jostii* RHA1 (Villalba & Alvarez, 2014). This Ltp1 transporter (ro05645) transports exogenous as well as endogenous long-chain fatty acids. These endogenous fatty acids probably originate from lipid membrane turnover or remodelling and fatty acid recycling. Ltp1 thus affects the distribution of the fatty acids between different metabolic pathways and lipid species (Villalba & Alvarez, 2014). The significantly lower abundance of Ltp1 in cells grown under TAG-accumulating conditions suggests that this transporter protein plays a role in lipid homeostasis predominantly during cell growth in *R. jostii* RHA1, modulating the distribution of lipids between metabolic pathways.

Additionally, the abundance of the L-ectoine synthase enzyme (ro01307), involved in the biosynthesis of ectoine, was 41.9-fold decreased in cells growing under TAG-accumulating conditions (Table 2). Ectoine is a compound synthesized by halophilic and halotolerant micro-organisms to prevent osmotic stress (Reshetnikov *et al.*, 2011). The biosynthesis of ectoine during desiccation was reported previously for *R. opacus* PD630 and *R. jostii* RHA1 (Alvarez *et al.*, 2004; LeBlanc *et al.*, 2008). Ectoine synthesis requires acetyl-CoA, glutamate and NADPH as precursors (Ofer *et al.*, 2012), which are also needed for the biosynthesis of TAGs. Thus, the high decrease in abundance of L-ectoine synthase during TAG accumulation suggested that the ectoine biosynthesis pathway competes with TAG synthesis for common intermediates and reducing equivalents. The partial inactivation of ectoine synthesis during TAG accumulation by *R. jostii* RHA1 may be part of the reorganization programme of cell metabolism.

Structural proteins of lipid bodies are upregulated under TAG-accumulating conditions

A protein highly synthesized by *R. jostii* RHA1 during TAG accumulation was ro02104 (2.3-fold), the homologue of

TadA from *R. opacus* PD630. This protein may play a structural role in the formation of lipid bodies, which resembles the role of apolipoproteins in eukaryotes (MacEachran *et al.*, 2010; Ding *et al.*, 2012). The protein encoded by the gene *ro02105*, annotated as a possible transcriptional regulator and located adjacent to the apolipoprotein, increased 2-fold in its abundance as well (Table 1). This regulatory protein may be involved in the modulation of the lipid body formation in *R. jostii* RHA1. However, the exact role of this regulatory component in TAG accumulation by rhodococci remains to be elucidated.

Amino acids are degraded under nitrogen-limiting/TAG-accumulating conditions to provide nitrogen, NADPH and precursors for TAG synthesis

During nitrogen-starvation-induced TAG synthesis and accumulation, 15 enzymes involved in the degradation of proteins and amino acids significantly increased their abundance (Table 1). The degradation of amino acids significantly contributes to the generation of metabolic energy (Fisher, 1999). Under nitrogen starvation conditions, such as they occur in the nitrogen-source-lacking MSM0, amino acids are presumably used by *R. jostii* RHA1 as an endogenous nitrogen source. Additionally, their degradation generates metabolic precursors to feed lipid biosynthesis pathways. The abundance of several enzymes involved in L-isoleucine and L-glutamate degradation pathways significantly increased under TAG-accumulating conditions (Table 1). In addition, the abundance of several (NADP$^+$)-dependent enzymes involved in the metabolism of other amino acids, such as ro01539, ro01542, ro00907 and ro01564, also increased during TAG accumulation by *R. jostii* RHA1 (Table 1).

Pathways generating propionyl-CoA, a precursor of odd-numbered fatty acids, are upregulated under TAG-accumulating conditions

The catabolism of L-isoleucine provides, in addition to acetyl-CoA, the metabolite propionyl-CoA, both of which can be used for the *de novo* fatty acid biosynthesis pathway (Fig. 4). Propionyl-CoA is generally used in the synthesis of odd-numbered fatty acids in rhodococci (Alvarez *et al.*, 1997). The fatty acid profile of *R. jostii* RHA1 revealed significant amounts of odd-numbered fatty acids (approx. 28 % of the total fatty acid content, Fig. 1). Previous studies demonstrated that rhodococci also utilize the methylmalonyl-CoA pathway for the production of propionyl-CoA. This pathway uses TCA cycle intermediates as precursors (Alvarez *et al.*, 1997; Feisthauer *et al.*, 2008). We observed an increased abundance of proteins involved in the methylmalonyl-CoA pathway, such as methylmalonyl-CoA mutase and propionyl-CoA carboxylase enzymes under TAG-accumulating conditions (Table 1, Fig. 4). Thus, both the methylmalonyl-CoA pathway and isoleucine degradation are contributing the propionyl-CoA
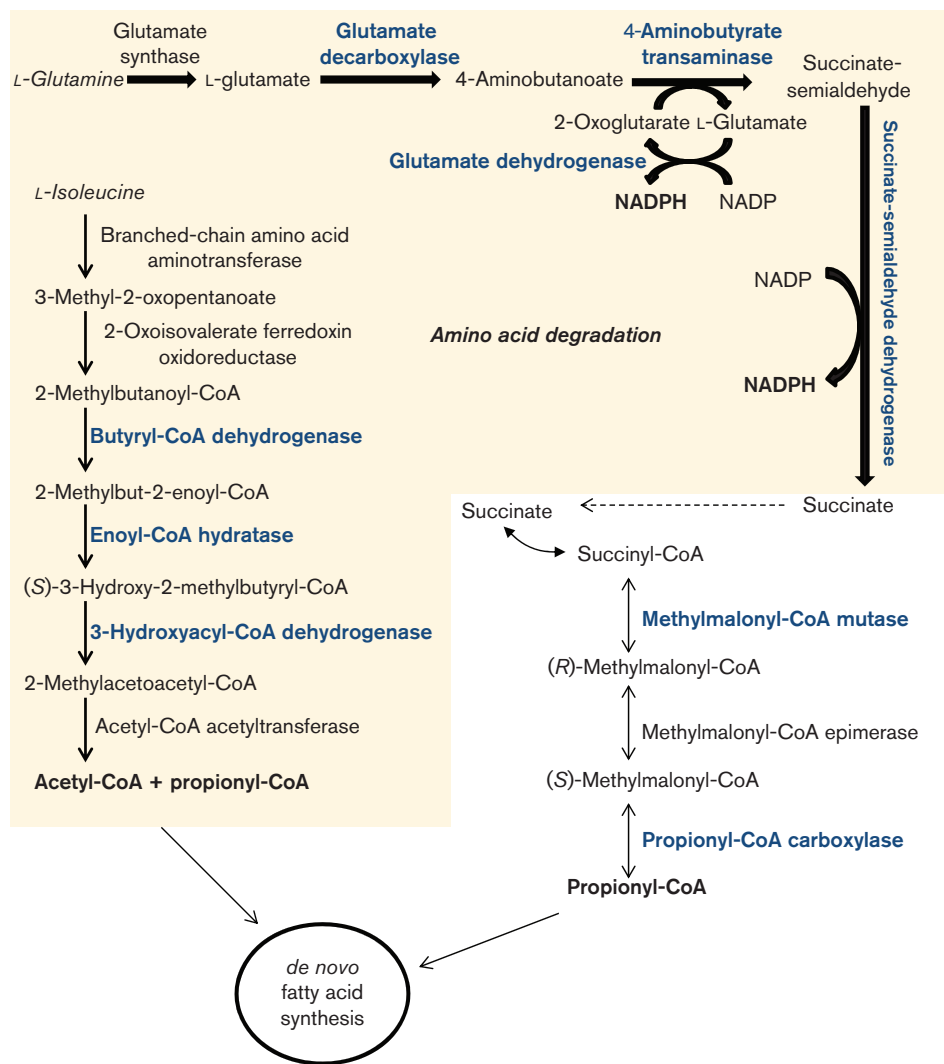
Fig. 4. Degradation of L-isoleucine and L-glutamate and the methylmalonyl-CoA pathway were activated during triacylglycerol biosynthesis in *R. jostii* RHA1. These pathways generate reductive power and precursors for the synthesis of even- and odd-numbered fatty acids. All enzymes were identified in the label-free proteome, but enzymes in blue showed significantly high abundance under TAG-accumulating conditions.

precursor to the biosynthesis of odd-numbered fatty acids. The degradation of ketogenic amino acids has been proposed as an alternative route for producing precursors for lipid biosynthesis in oleaginous yeasts and fungi (Vorapreeda *et al.*, 2012). Additionally, enzymes involved in L-glutamate degradation to the TCA intermediate succinate significantly increased in abundance during TAG-accumulating conditions (Table 1, Fig. 4). In addition to the generation of reductive power for the synthesis of fatty acids, succinate serves as a precursor for the methylmalonyl-CoA pathway for the biosynthesis of odd-numbered fatty acids, and can enter into glyceroneogenesis for the production of glycerol 3-phosphate (Fig. 4). Genes encoding methylmalonyl-CoA mutase and propionyl-CoA carboxylase were also significantly induced in *R. opacus* PD630 during TAG accumulation

(Chen *et al.*, 2014). Like *R. jostii* RHA1, *R. opacus* PD630 is able to produce odd-numbered fatty acids during growth with gluconate or glucose (Alvarez *et al.*, 1996).

R. jostii expresses proteins to access alternative nitrogen sources in ammonium-chloride-lacking medium MSM0

We also observed an increase in abundance of amino acid transporters in *R. jostii* RHA1 cells during TAG accumulation (Table 1). The induction of several amino acid transporters in *R. jostii* RHA1 under these nitrogen starvation conditions may allow cells the uptake of alternative nitrogen sources from the environment. In the related oleaginous *R. opacus* PD630, several genes related to amino acid degradation and

transport were also highly expressed 3 h after cells were transferred to TAG-accumulation conditions (Chen *et al.*, 2014). In our study, *R. jostii* RHA1 cells significantly increased the abundance of key proteins of nitrogen metabolism when grown under TAG-accumulating conditions (Table 1). Cells expressed proteins responsible for nitrogen uptake, assimilation and regulation, including several ammonium transporters, enzymes for nitrate or nitrite reduction and cleavage of nitrogen sources (urease complex), among others. Regulatory proteins involved in the control of nitrogen metabolism (Amin *et al.*, 2012), such as GlnB (ro06531) and GlnD (ro06532), increased their abundance 11.1- and infinity-fold, respectively, in media lacking nitrogen sources compared with medium containing ammonium chloride (Table 1). The global regulator GlnR, which plays a central role in the transcriptional regulation of genes involved in nitrogen metabolism in bacteria, was present in both media with similar abundance. Activity of this protein, however, is regulated post-translationally by phosphorylation (Barton *et al.*, 2013).

Redox proteome reveals that some proteins are slightly oxidized in MSM1

Oleaginous micro-organisms such as *R. jostii* RHA1 need a high level of reducing power for supporting a high ratio of lipid biosynthesis during TAG accumulation. Synthesis of one molecule of palmitic acid ($C_{16:0}$) from eight molecules of acetyl-CoA requires 14 molecules of NADPH and seven molecules of ATP. In this study, we observed the activation of several NADPH-dependent enzymatic reactions during TAG accumulation in *R. jostii* RHA1. Many of these enzymes possess cysteines in their primary structure. To examine if these cysteines are susceptible to oxidation by reactive oxygen species, we analysed *R. jostii* RHA1's thiol redox proteome in the presence and absence of the pro-oxidant methyl viologen during TAG accumulation. Methyl viologen (paraquat) is thought to produce superoxide within the cell through an enzymic redox cycling mechanism. To analyse the redox proteome, we used the MS-based OxICAT method, which uses thiol-specific isotopic labels to determine the ratio of the reduced and oxidized fraction (Leichert *et al.*, 2008; Brandes *et al.*, 2011; Lindemann *et al.*, 2013).

A small group of proteins prone to oxidation was identified with OxICAT as shown in Table 3. Two of those enzymes, fructose-bisphosphate aldolase and fructose 1,6-bisphosphatase involved in glycolysis and gluconeogenesis, showed higher oxidation. Fructose-bisphosphate aldolase has been identified previously as a redox-sensitive protein partially oxidized when *S. cerevisiae* cells were exposed to H_2O_2 (Brandes *et al.*, 2011). The authors suggested that prevailing redox conditions constantly control central cellular pathways by fine-tuning oxidation status and hence activity of proteins. Fructose 1,6-bisphosphatase and fructose-bisphosphate aldolase also increased in abundance to some extent in *R. jostii* RHA1 under TAG-accumulating conditions. Our

results suggest that activity of these enzymes is not only regulated on the expression level and by phosphorylation, but might also be finely regulated by the redox status of cells.

Two enzymes, β-ketoacyl-[ACP] synthase II (FabF) and β-ketoacyl-[ACP] reductase (FabG), which are components of the FAS-II system were also identified in the redox proteome (Table 3). FAS-II is a multi-enzyme complex that elongates the acyl-CoA primers generated by FAS-I to produce mycolic acids (Bhatt *et al.*, 2007). The abundance of FabF and FabG was also increased during TAG accumulation by *R. jostii* RHA1 as shown in Table 1. The percentage of oxidized cysteine in FabF was higher in MSM1 and MSM0 + MV. FabF is involved in the condensation reaction; thus, the oxidized cysteine detected in MSM1 may be due to the thio-ester intermediate formed during the synthesis of mycolic acid. This is consistent with the fact that cells need to synthesize mycolic acid during the exponential phase of growth. A similar percentage of oxidized cysteine was detected in MSM0 + MV (low TAG accumulation). Recent studies demonstrated that the β-ketoacyl-[ACP] synthase II (FabF) present in *E. coli*, is a redox-sensitive protein, which is substantially oxidized in the presence of an oxidant (Brandes *et al.*, 2007). This protein possesses a highly conserved cysteine within its catalytic site (C164). Brandes *et al.* (2007) postulated that modification of this active-site cysteine may substantially interrupt fatty acid synthesis in bacteria. Interestingly, the redox-modified cysteine is located in the conserved region of the active site of FabF from *R. jostii* RHA1 as revealed by the sequence alignment with FabF from *E. coli* (Fig. S3). Regarding FabG, a higher percentage of oxidized cysteine was only detected in the presence of paraquat. FabF from *R. jostii* RHA1, and probably FabG to some extent, might be enzymes potentially controlled by redox-modifications. The FAS-II system and TAG biosynthesis require the acyl-CoA pool generated by the FAS-I system. The high abundance of FAS-II components detected in MSM0 (Table 1) might occur in response to competition with the TAG biosynthesis pathway since at the sampling point for proteomics studies, cells still exhibited growth in MSM0 (Fig. S1).

In addition, we identified an acetyl/propionyl-CoA carboxylase (alpha subunit) encoded by the gene *ro04222*, which is one of the most abundant proteins found in cells in MSM1 as well as in MSM0 (Tables 3 and S1). Acetyl-CoA carboxylase (ACCase) catalyses the first committed step of *de novo* fatty acid synthesis, converting acetyl-CoA and CO_2 to malonyl-CoA by using ATP (Liang & Jiang, 2013). *ro04222* (1828 aa; EC 6.3.4.14) catalyses the same reaction as the redox-sensitive ACCase protein (2232 aa; EC 6.3.4.14) of *S. cerevisiae* (Brandes *et al.*, 2011). This enzyme is a key-regulatory step in fatty acid biosynthesis and its activity can be redox-controlled in eukaryotic organisms including plants and yeast (Geigenberger *et al.*, 2005; Brandes *et al.*, 2011). Our label-free proteome analysis revealed that the abundance of *ro04222* increased 1.9-fold in MSM0. Altogether, our results suggested that this rhodococcal ACCase may be involved in fatty acid biosynthesis in

Table 3. Thiol-oxidation of cysteines identified in MSM0, MSM1 and MSM0 supplemented with methyl viologen (MSM0 + MV)

Peptide	Protein	Oxidation (%)			Gene
		MSM0	MSM1	MSM0 + MV	
KASPSDVTV**C**ILDRPR	Fructose 1,6-bisphosphatase	17	31	22	RHA1_ro05865
AGVITPVSA**C**SSGSEAIAHAYR	β-Ketoacyl-[ACP] synthase II. 'FabF'	34	41	43	RHA1_ro01201
DGAHVI**C**ADIPAAGEALSETANK	β-Ketoacyl-[ACP] reductase. 'FabG'	21	nd	38	RHA1_ro05199
AA**C**DVLAPQFEASHGVDGR	Transaldolase	16	25	22	RHA1_ro07185
AKEHSFAFPAIN**C**TSSETINAAIK	Fructose-bisphosphate aldolase	23	31	33	RHA1_ro05536
GEFDHLPEQAFNS**C**GGLDDVEAAAK	H(+)-transporting two-sector ATPase beta subunit	39	67	35	RHA1_ro01472
LASDAGGVLV**C**R	dUTPase	17	54	45	RHA1_ro06827
LVGGQHPTAVLFG**C**GDSR	Carbonate dehydratase	33	50	46	RHA1_ro04449
VALFGDPTKALGTVAEAE**C**AR	Probable acetyl/propionyl-CoA carboxylase alpha subunit	10	15	19	RHA1_ro04222
SHPGVTATF**C**EALAK	Aspartate kinase	17	27	25	RHA1_ro04291
MSVGPMDNNVYLVV**C**SATGK	Zn-dependent hydrolase	10	21	17	RHA1_ro00970

nd, not detected.

R. jostii RHA1 and its activity may be controlled at the transcriptional level, but may also be finely modulated by the redox status of the cell.

The OxiCAT methodology allowed us to identify some proteins prone to redox-modification which are involved in carbohydrate and lipid metabolism in *R. jostii* RHA1. Apparently, these proteins possess allosteric disulfide bonds, which control their activity depending on the oxidation status of the cysteines (Azimi *et al.*, 2011). This analysis is expected to help the orientation of further studies to determine which proteins involved in TAG metabolism undergo reversible thiol modifications in response to changes in the redox status of rhodococcal cells. To our knowledge this is the first report in which a redox proteomic approach has been applied for studying oleaginous bacteria.

CONCLUSION

The most salient features of TAG-accumulating cells of *R. jostii* RHA1 include (i) the activation of metabolic pathways such as the pentose phosphate pathway and the Entner–Duodoroff pathway, which generate reducing equivalents and precursors for lipid biosynthesis, (ii) activation of gluconeogenic reactions and glycogen mobilization, (iii) TAG recycling, (iv) activation of glyceroneogenesis, as well as GlpD and GpsA enzymes, which seem to work together to regulate availability of glycerol 3-phosphate, (v) increase of catabolic enzymes of amino acids for generating acetyl-CoA, propionyl-CoA and NADPH, (vi) inhibition of enzymes of the L-ectoine biosynthesis pathway, which consumes acetyl-CoA and NADPH, and (vii) activation of the lipid biosynthesis machinery and the induction of the structural proteins necessary for formation of lipid bodies. Finally, some key enzymes of the central and lipid metabolism seem to be regulated not only at a transcriptional level, but also by

the variation of the redox status of cells, such as the highly abundant ACCase, FabF and fructose 1,6 bisphosphatase.

REFERENCES

Alvarez, H. M. & Steinbüchel, A. (2010). Physiology, biochemistry and molecular biology of triacylglycerol accumulation by *Rhodococcus*. In *Biology of Rhodococcus* (Microbiology Monographs vol. 16), pp. 263–290. Edited by H. M. Alvarez. Heidelberg: Springer.

Alvarez, H. M., Mayer, F., Fabritius, D. & Steinbüchel, A. (1996). Formation of intracytoplasmic lipid inclusions by *Rhodococcus opacus* strain PD630. *Arch Microbiol* **165**, 377–386.

Alvarez, H. M., Kalscheuer, R. & Steinbüchel, A. (1997). Accumulation of storage lipids in species of *Rhodococcus* and *Nocardia* and effect of inhibitors and polyethylene glycol. *Fett/Lipid* **99**, 239–246.

Alvarez, H. M., Kalscheuer, R. & Steinbüchel, A. (2000). Accumulation and mobilization of storage lipids by *Rhodococcus opacus* PD630 and *Rhodococcus ruber* NCIMB 40126. *Appl Microbiol Biotechnol* **54**, 218–223.

Alvarez, H. M., Silva, R. A., Cesari, A. C., Zamit, A. L., Peressutti, S. R., Reichelt, R., Keller, U., Malkus, U., Rasch, C. & other authors (2004). Physiological and morphological responses of the soil bacterium *Rhodococcus opacus* strain PD630 to water stress. *FEMS Microbiol Ecol* **50**, 75–86.

Alvarez, A. F., Alvarez, H. M., Kalscheuer, R., Wältermann, M. & Steinbüchel, A. (2008). Cloning and characterization of a gene involved in triacylglycerol biosynthesis and identification of additional homologous genes in the oleaginous bacterium *Rhodococcus opacus* PD630. *Microbiology* **154**, 2327–2335.

Alvarez, H. M., Silva, R. A., Herrero, M., Hernández, M. A. & Villalba, M. S. (2012). Metabolism of triacylglycerols in *Rhodococcus* species: insights from physiology and molecular genetics. *J Mol Biochem* **2**, 69–78.

Amin, R., Reuther, J., Bera, A., Wohlleben, W. & Mast, Y. (2012). A novel GlnR target gene, nnaR, is involved in nitrate/nitrite assimilation in *Streptomyces coelicolor*. *Microbiology* **158**, 1172–1182.

Azimi, I., Wong, J. W. & Hogg, P. J. (2011). Control of mature protein function by allosteric disulfide bonds. *Antioxid Redox Signal* **14**, 113–126.

Barney, B. M., Wahlen, B. D., Garner, E., Wei, J. & Seefeldt, L. C. (2012). Differences in substrate specificities of five bacterial wax ester synthases. *Appl Environ Microbiol* **78**, 5734–5745.

Barton, M. D., Petronio, M., Giarrizzo, J. G., Bowling, B. V. & Barton, H. A. (2013). The genome of *Pseudomonas fluorescens* strain R124 demonstrates phenotypic adaptation to the mineral environment. *J Bacteriol* **195**, 4793–4803.

Bequer Urbano, S., Albarracín, V. H., Ordoñez, O. F., Farías, M. E. & Alvarez, H. M. (2013). Lipid storage in high-altitude Andean Lakes extremophiles and its mobilization under stress conditions in *Rhodococcus* sp. A5, a UV-resistant actinobacterium. *Extremophiles* **17**, 217–227.

Bhatt, A., Molle, V., Besra, G. S., Jacobs, W. R., Jr & Kremer, L. (2007). The *Mycobacterium tuberculosis* FAS-II condensing enzymes: their role in mycolic acid biosynthesis, acid-fastness, pathogenesis and in future drug development. *Mol Microbiol* **64**, 1442–1454.

Brandes, N., Rinck, A., Leichert, L. I. & Jakob, U. (2007). Nitrosative stress treatment of *E. coli* targets distinct set of thiol-containing proteins. *Mol Microbiol* **66**, 901–914.

Brandes, N., Reichmann, D., Tienson, H., Leichert, L. I. & Jakob, U. (2011). Using quantitative redox proteomics to dissect the yeast redoxome. *J Biol Chem* **286**, 41893–41903.

Chen, B. S., Otten, L. G., Resch, V., Muyzer, G. & Hanefeld, U. (2013). Draft genome sequence of *Rhodococcus rhodochrous* strain ATCC 17895. *Stand Genomic Sci* **9**, 175–184.

Chen, Y., Ding, Y., Yang, L., Yu, J., Liu, G., Wang, X., Zhang, S., Yu, D., Song, L. & other authors (2014). Integrated omics study delineates the dynamics of lipid droplets in *Rhodococcus opacus* PD630. *Nucleic Acids Res* **42**, 1052–1064.

Chubukov, V., Gerosa, L., Kochanowski, K. & Sauer, U. (2014). Coordination of microbial metabolism. *Nat Rev Microbiol* **12**, 327–340.

Cox, J. & Mann, M. (2008). MaxQuant enables high peptide identification rates, individualized p.p.b.-range mass accuracies and proteome-wide protein quantification. *Nat Biotechnol* **26**, 1367–1372.

Cox, J., Neuhauser, N., Michalski, A., Scheltema, R. A., Olsen, J. V. & Mann, M. (2011). Andromeda: a peptide search engine integrated into the MaxQuant environment. *J Proteome Res* **10**, 1794–1805.

Desvergne, B., Michalik, L. & Wahli, W. (2006). Transcriptional regulation of metabolism. *Physiol Rev* **86**, 465–514.

Ding, Y., Yang, L., Zhang, S., Wang, Y., Du, Y., Pu, J., Peng, G., Chen, Y., Zhang, H. & other authors (2012). Identification of the major functional proteins of prokaryotic lipid droplets. *J Lipid Res* **53**, 399–411.

Feisthauer, S., Wick, L. Y., Kästner, M., Kaschabek, S. R., Schlömann, M. & Richnow, H. H. (2008). Differences of heterotrophic

13CO2 assimilation by *Pseudomonas knackmussii* strain B13 and *Rhodococcus opacus* 1CP and potential impact on biomarker stable isotope probing. *Environ Microbiol* **10**, 1641–1651.

Fisher, S. H. (1999). Regulation of nitrogen metabolism in *Bacillus subtilis*: vive la différence! *Mol Microbiol* **32**, 223–232.

Gago, G., Diacovich, L., Arabolaza, A., Tsai, S. C. & Gramajo, H. (2011). Fatty acid biosynthesis in actinomycetes. *FEMS Microbiol Rev* **35**, 475–497.

Geigenberger, P., Kolbe, A. & Tiessen, A. (2005). Redox regulation of carbon storage and partitioning in response to light and sugars. *J Exp Bot* **56**, 1469–1479.

Hanson, R. W. & Reshef, L. (2003). Glyceroneogenesis revisited. *Biochimie* **85**, 1199–1205.

Hernández, M. A., Mohn, W. W., Martínez, E., Rost, E., Alvarez, A. F. & Alvarez, H. M. (2008). Biosynthesis of storage compounds by *Rhodococcus jostii* RHA1 and global identification of genes involved in their metabolism. *BMC Genomics* **9**, 600.

Hernández, M. A., Arabolaza, A., Rodríguez, E., Gramajo, H. & Alvarez, H. M. (2013). The atf2 gene is involved in triacylglycerol biosynthesis and accumulation in the oleaginous *Rhodococcus opacus* PD630. *Appl Microbiol Biotechnol* **97**, 2119–2130.

Hernández, M. A., Comba, S., Arabolaza, A., Gramajo, H. & Alvarez, H. M. (2014). Overexpression of a phosphatidic acid phosphatase type 2 leads to an increase in triacylglycerols production in oleaginous Rhodococcus strains. *Appl. Microbiol. Biotechnol.* DOI: 10.1007/s00253-014-6002-2

Iddar, A., Valverde, F., Assobhei, O., Serrano, A. & Soukri, A. (2005). Widespread occurrence of non-phosphorylating glyceraldehyde-3-phosphate dehydrogenase among gram-positive bacteria. *Int Microbiol* **8**, 251–258.

Kumsta, C., Thamsen, M. & Jakob, U. (2011). Effects of oxidative stress on behavior, physiology, and the redox thiol proteome of *Caenorhabditis elegans*. *Antioxid Redox Signal* **14**, 1023–1037.

Le Bihan, T., Rayner, J., Roy, M. M. & Spagnolo, L. (2013). *Photobacterium profundum* under pressure: a MS-based label-free quantitative proteomics study. *PLoS ONE* **8**, e60897.

LeBlanc, J. C., Gonçalves, E. R. & Mohn, W. W. (2008). Global response to desiccation stress in the soil actinomycete *Rhodococcus jostii* RHA1. *Appl Environ Microbiol* **74**, 2627–2636.

Leichert, L. I. (2011). Proteomic methods unravel the protein quality control in *Escherichia coli*. *Proteomics* **11**, 3023–3035.

Leichert, L. I., Gehrke, F., Gudiseva, H. V., Blackwell, T., Ilbert, M., Walker, A. K., Strahler, J. R., Andrews, P. C. & Jakob, U. (2008). Quantifying changes in the thiol redox proteome upon oxidative stress *in vivo*. *Proc Natl Acad Sci U S A* **105**, 8197–8202.

Liang, M. H. & Jiang, J. G. (2013). Advancing oleaginous microorganisms to produce lipid via metabolic engineering technology. *Prog Lipid Res* **52**, 395–408.

Lindemann, C. & Leichert, L. I. (2012). Quantitative redox proteomics: the NOxICAT method. *Methods Mol Biol* **893**, 387–403.

Lindemann, C., Lupilova, N., Müller, A., Warscheid, B., Meyer, H. E., Kuhlmann, K., Eisenacher, M. & Leichert, L. I. (2013). Redox proteomics uncovers peroxynitrite-sensitive proteins that help *Escherichia coli* to overcome nitrosative stress. *J Biol Chem* **288**, 19698–19714.

Liu, X., Hu, Y., Pai, P. J., Chen, D. & Lam, H. (2014). Label-free quantitative proteomics analysis of antibiotic response in *Staphylococcus aureus* to oxacillin. *J Proteome Res* **13**, 1223–1233.

MacEachran, D. P. & Sinskey, A. J. (2013). The *Rhodococcus opacus* TadD protein mediates triacylglycerol metabolism by regulating intracellular NAD(P)H pools. *Microb Cell Fact* **12**, 104.

MacEachran, D. P., Prophete, M. E. & Sinskey, A. J. (2010). The *Rhodococcus opacus* PD630 heparin-binding hemagglutinin homolog TadA mediates lipid body formation. *Appl Environ Microbiol* **76**, 7217–7225.

McLeod, M. P., Warren, R. L., Hsiao, W. W., Araki, N., Myhre, M., Fernandes, C., Miyazawa, D., Wong, W., Lillquist, A. L. & other authors (2006). The complete genome of *Rhodococcus* sp. RHA1 provides insights into a catabolic powerhouse. *Proc Natl Acad Sci U S A* **103**, 15582–15587.

Mráček, T., Drahota, Z. & Houštěk, J. (2013). The function and the role of the mitochondrial glycerol-3-phosphate dehydrogenase in mammalian tissues. *Biochim Biophys Acta* **1827**, 401–410.

Müller, A., Hoffmann, J. H., Meyer, H. E., Narberhaus, F., Jakob, U. & Leichert, L. I. (2013). Nonnative disulfide bond formation activates the σ32-dependent heat shock response in *Escherichia coli*. *J Bacteriol* **195**, 2807–2816.

Ofer, N., Wishkautzan, M., Meijler, M., Wang, Y., Speer, A., Niederweis, M. & Gur, E. (2012). Ectoine biosynthesis in *Mycobacterium smegmatis*. *Appl Environ Microbiol* **78**, 7483–7486.

Reshetnikov, A. S., Khmelenina, V. N., Mustakhimov, I. I., Kalyuzhnaya, M., Lidstrom, M. & Trotsenko, Y. A. (2011). Diversity and phylogeny of the ectoine biosynthesis genes in aerobic, moderately halophilic methylotrophic bacteria. *Extremophiles* **15**, 653–663.

Schlegel, H. G., Kaltwasser, H. & Gottschalk, G. (1961). [A submersion method for culture of hydrogen-oxidizing bacteria: growth physiological studies]. *Arch Mikrobiol* **38**, 209–222 (in German).

Smith, S., Witkowski, A. & Joshi, A. K. (2003). Structural and functional organization of the animal fatty acid synthase. *Prog Lipid Res* **42**, 289–317.

Sutcliffe, I. C., Brown, A. K. & Dover, L. G. (2010). The rhodococcal cell envelope: composition, organisation and biosynthesis. In *Biology of Rhodococcus* (Microbiology Monographs vol. 16), pp. 29–71. Edited by H. M. Alvarez. Heidelberg: Springer.

Villalba, M. S. & Alvarez, H. M. (2014). Identification of a novel ATP-binding cassette transporter involved in long-chain fatty acid import and its role in triacylglycerol accumulation in *Rhodococcus jostii* RHA1. *Microbiology* **160**, 1523–1532.

Villalba, M. S., Hernández, M. A., Silva, R. A. & Alvarez, H. M. (2013). Genome sequences of triacylglycerol metabolism in *Rhodococcus* as a platform for comparative genomics. *J Mol Biochem* **2**, 94–105.

Vorapreeda, T., Thammarongtham, C., Cheevadhanarak, S. & Laoteng, K. (2012). Alternative routes of acetyl-CoA synthesis identified by comparative genomic analysis: involvement in the lipid production of oleaginous yeast and fungi. *Microbiology* **158**, 217–228.

Edited by: Y. Ohnishi